Bull Volcanol (2005) 67:457–468
DOI 10.1007/s00445-004-0387-1

RESEARCH ARTICLE

Alexander Belousov · Thomas R. Walter · Valentin R. Troll

Large-scale failures on domes and stratocones situated on caldera ring faults: sand-box modeling of natural examples from Kamchatka, Russia

Received: 5 June 2003 / Accepted: 18 August 2004 / Published online: 20 November 2004

Abstract Edifices of stratocones and domes are often situated eccentrically above shallow silicic magma reservoirs. Evacuation of such reservoirs forms collapse calderas commonly surrounded by remnants of one or several volcanic cones that appear variously affected and destabilized. We studied morphologies of six calderas in Kamchatka, Russia, with diameters of 4 to 12 km. Edifices affected by caldera subsidence have residual heights of 250–800 m, and typical amphitheater-like depressions opening toward the calderas. The amphitheaters closely resemble horseshoe-shaped craters formed by large-scale flank failures of volcanoes with development of debris avalanches. Where caldera boundaries intersect such cones, the caldera margins have notable outward embayments. We therefore hypothesize that in the process of caldera formation, these eccentrically situated edifices were partly displaced and destabilized, causing large-scale landslides. The landslide masses are then transformed into debris avalanches and emplaced inside the developing caldera basins. To test this hypothesis, we carried out sand-box analogue experiments, in which caldera formation (modeled by evacuation of a rubber balloon) was simulated. The deformation of volcanic cones was studied by placing sand-cones in the vicinity of the expected "caldera" rim. At the initial stage of the modeled subsidence, the propagating ring fault of the caldera bifurcates within the affected cone into two faults, the outermost of which is notably curved outward off the caldera center. The two faults dissect the cone into three parts: (1) a stable outer part, (2) a highly unstable and subsiding intracaldera part, and (3) a subsiding graben structure between parts (1) and (2). Further progression of the caldera subsidence is likely to cause failure of parts (2) and (3) with failed material sliding into the caldera basin and with formation of an amphitheater-like depression oriented toward the developing caldera. The mass of material which is liable to slide into the caldera basin, and the shape of the resulted amphitheater are a function of the relative position of the caldera ring fault and the base of the cone. A cone situated mostly outside the ring fault is affected to a minor degree by caldera subsidence and collapses with formation of a narrow amphitheater deeply incised into the cone, having a small opening angle. Accordingly, the caldera exhibits a prominent outward embayment. By contrast, collapse of a cone initially situated mostly inside the caldera results in a broad amphitheater with a large opening angle, i.e. the embayment of the caldera rim is negligible. The relationships between the relative position of an edifice above the caldera fault and the opening angle of the formed amphitheater are similar for the modeled and the natural cases of caldera/cone interactions. Thus, our experiments support the hypothesis that volcanic edifices affected by caldera subsidence can experience large-scale failures with formation of indicative amphitheaters oriented toward the caldera basins. More generally, the scalloped appearance of boundaries of calderas in contact with pre-caldera topographic highs can be explained by the gravitational influence of topography on the process of caldera formation.

Keywords Caldera subsidence · Volcano instability · Large-scale landslides · Debris avalanche

Editorial responsibility: J. Stix

A. Belousov
Institute of Marine Geology and Geophysics,
Yuzhno-Sakhalinsk, Russia and Institute of Volcanology and Seismology,
Petropavlovsk-Kamchatsky, Russia

T. R. Walter (✉)
MGG/RSMAS,
University of Miami,
4600 Rickenbacker Cswy, FL 33149, USA
e-mail: twalter@rsmas.miami.edu

V. R. Troll
Dept. of Geology,
Trinity College, College Green,
Dublin 2, Ireland

Introduction

Analogue modeling is widely used to test interpretations of volcanic processes derived from geological data and provide insight into the basic operating mechanisms. In this paper, we present the results of analogue sand-box modeling of two volcanic phenomena which were previously modeled independently but never examined in the framework of one interrelated scenario: caldera subsidence and associated disruption of volcanic cones.

Caldera-forming eruptions are among the most impressive manifestations of volcanic activity on Earth (e.g. Newhall and Dzurisin 1988). Formation of a large, 10-km diameter or more caldera is a rather rare event and satisfactory observations are absent. Some available observational data have been obtained on several historic eruptions with formation of relatively small calderas (Simkin and Fiske 1983; Newhall and Punongbayan 1996). Thus geological data and modeling are the main sources of information about the process of caldera formation. Geological data have shown that ash-flow calderas are the result of subsidence of roofs of large silicic magma chambers evacuated during voluminous eruptions of ignimbrites (Williams 1941; Druitt and Sparks 1984; Francis 1993). The process of caldera subsidence has been modeled experimentally by a range of workers (e.g. Komuro 1987; Marti et al. 1994; Branney 1995; Roche et al. 2000; Walter and Troll 2001; Acocella et al. 2001; Troll et al. 2002; Kennedy et al. 2004) who showed that caldera subsidence occurs mainly along outward-dipping ring faults that allow subsidence of the central caldera floor either as a piston, trapdoor, funnel or in piecemeal fashion. In these experiments, for simplicity, the ground surface above magma chambers was considered as either flat, i.e., no relief, or as a single cone placed directly above the magma chamber. In reality, the ground surface above large magma chambers commonly shows complex irregularities such as one or several volcanic edifices (stratocones and/or domes) that were formed during the pre-caldera history of these magmatic systems. The cones and domes are located eccentrically and/or directly above the magma chamber. The presence of such relief could have two consequences. Firstly, due to gravitational loading, a volcanic cone changes the stress field in the vicinity of a shallow magma chamber and could notably influence magma chamber stability (e.g. Pinel and Jaupard 2003) and caldera formation, ie. such as the orientation of caldera faults and type of subsidence of the roof into the magma chamber. This influence of pre-existing topography for caldera fault development was recently studied by analogue experiments (Walter and Troll 2001; Lavallée et al. 2004), highlighting that the topography may influence or even control the style of caldera subsidence. Secondly, if a caldera fault crosses a volcanic edifice, the structural instability that is induced can lead to large-scale landslides. Intersection of volcanic cones by tectonic faults was investigated experimentally by Vidal and Merle (2000). In their experiments, instability of the volcanic edifice was induced by formation of faults in the volcano's substrate. The experiments revealed that stratocones situated above a reactivated normal fault will be ruptured and can be divided structurally into three domains: a stable external part on the footwall block, an unstable part on the hanging wall, and a central wedge-like graben in-between. These experiments confirmed the idea that movements along tectonic faults in the substrate of a volcano could lead to failure of the volcanic cone. Such a scenario has the potential to generate massive landslides. However, the quantitative evaluation of the landslide potential, particularly in relation to the fault position underneath such a cone, is still unclear. For example, the vertical displacement in these experiments that produced an analogue landslide would be unrealistically large (~400 m) for pure tectonic motions (cf. Vidal and Merle 2000). The authors suggested that such a large displacement necessary to generate failure could be accumulated over a long period of time (many thousands of years) as a result of multiple small displacements. But it is also probable that an active volcano will rebuild and thus "repair" itself during this period, compensating for this type of destabilization. Alternatively, the edifice of an inactive volcano will be almost completely eroded away. Displacements of several hundred meters magnitude can be achieved by caldera faults. Thus, this mechanism of destabilization is applicable to volcanic edifices situated in the vicinities of developing calderas. Examination of several large calderas on the Kamchatka Peninsula, Russia, suggests such a process to be rather common. Many volcanic cones on the boundaries of younger large calderas were affected by caldera subsidence to various degrees and display horseshoe-shaped morphologies typical for volcanoes that have experienced large-scale flank failures (Siebert 1984).

Natural examples of caldera/cone interaction from Kamchatka

The six studied calderas are situated in the central part of the Eastern Volcanic Belt of Kamchatka Peninsula, Russia (Fig. 1). The calderas, ranging from 4 to 12 km in diameter, were formed in the Late Pleistocene–Early Holocene, associated with voluminous eruptions of silicic ignimbrites (Piip 1961; Ivanov 1970; Selyangin 1987; Leonov et al. 1991; Ivanov et al. 1991; Braitseva et al. 1995). Due to the relatively young ages of the calderas, their escarpments are well defined and the caldera boundaries easily outlined on topographic maps and aerial images.

Escarpments of the calderas crosscut several moderate-sized volcanic cones of mostly basalt–basaltic andesite composition (Figs. 2 and 3). The cones were formed before the adjacent calderas in the Late Pliocene–Early Pleistocene (Ivanov 1970; Selyangin 1987; Leonov et al. 1991). There are no data to show that the affected volcanoes were active during or after the caldera-forming eruptions. At the time of caldera formation, the evacuating magma reservoir was located not underneath but ec-

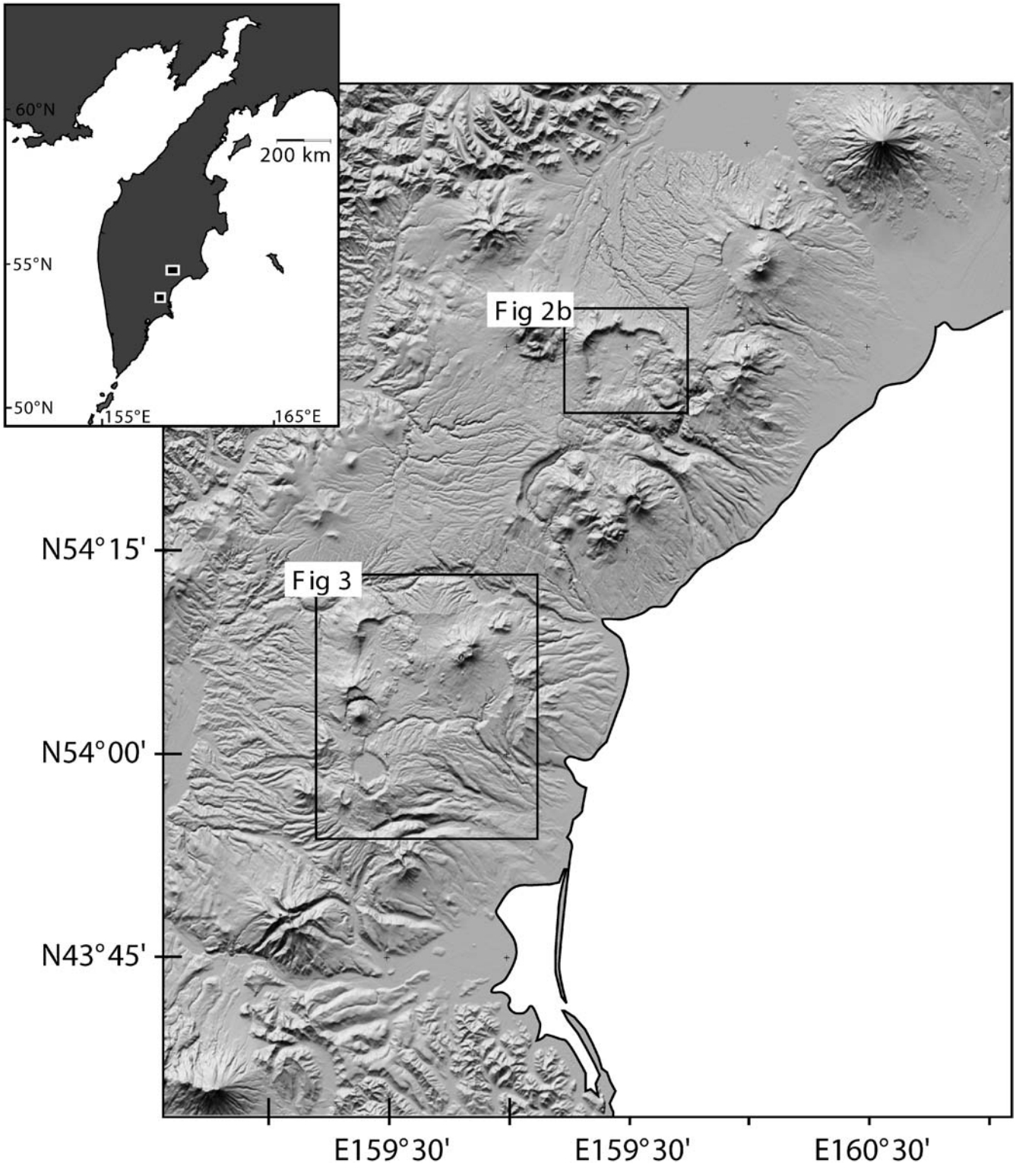

Fig. 1 Shaded relief map of the studied part of the Eastern Volcanic Ridge of Kamchatka, where numerous calderas are found. *Squares* show areas enlarged in Figs. 2b and 3. Locations of the areas are shown on the insert map of Kamchatka Peninsula. Shaded relief generated from digital elevation data by Shuttle radar topography mission (SRTM)

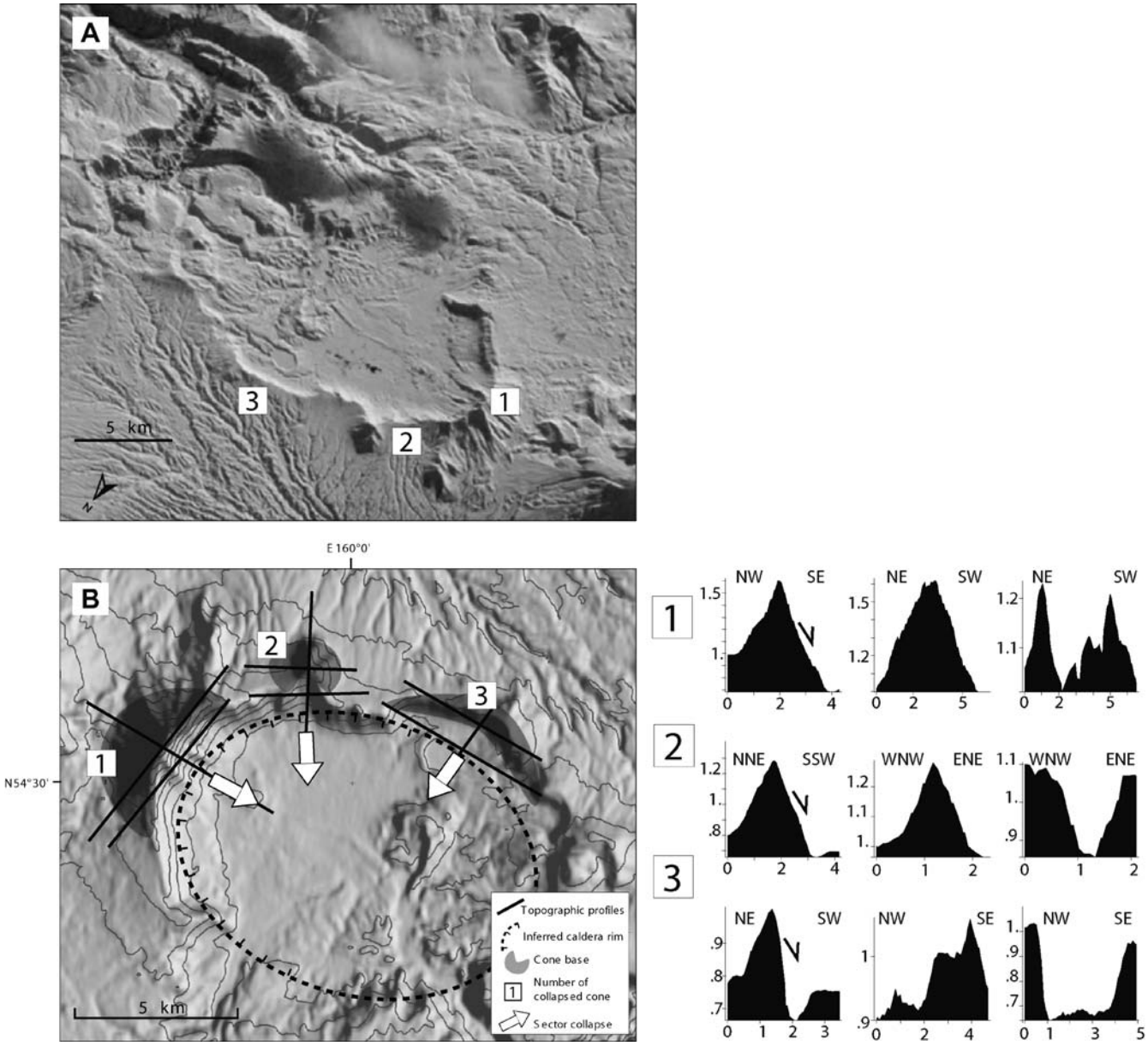

Fig. 2 **A** Perspective hand-held space shuttle photograph of Uzon caldera (6×9 km). The rim of the caldera has a scalloped appearance with notable outward embayments where it crosses pre-caldera cones. *Numbers* indicate remnants of collapsed volcanic edifices: *1* Uzon, *2* Krasnaya Sopka, *3* Ozernaya Sopka. Image courtesy of Earth Sciences and Image Analysis Laboratory, NASA, Johnson Space Center. **B** Shaded relief map of Uzon caldera and topographic profiles through volcanoes located on the caldera boundary. Boundary of the caldera is shown schematically as a *circle* to highlight embayments of the caldera into the pre-caldera cones. Names of volcanoes around Uzon caldera: *1* Uzon, *2* Krasnaya Sopka, *3* Ozernaya Sopka. Location of the area is shown on Fig. 1. Topographic profiles from left to right: in the direction of failure; transverse through the amphitheater's head; transverse through the amphitheater's breach; numbers are in km. *Arrows* indicate directions of the deduced failures of the pre-caldera cones. Characteristics of the cones are summarized in Table 1. DEM from SRTM data, 100-m topographic isolines

centric to the volcanic cones. During collapse of the calderas, these preexisting cones were dissected to various degrees by the caldera faults, thus causing different degrees of cone destruction.

The intersections of the cones and the calderas resulted in peculiar morphological features of both. All the affected cone edifices have amphitheater-like depressions opening toward the corresponding caldera basins. Accordingly, the escarpments of the calderas developed notable outward embayments where they intersect the cones. Morphological similarities of the amphitheaters to typical horseshoe-shaped landslide craters (e.g. Siebert 1984) suggest that during caldera subsidence the eccentrically situated edifices probably experienced large-scale landslides. The landslide masses transformed into debris avalanches and were emplaced inside the basin of the developing caldera. Since these debris avalanches were deposited inside the calderas, their deposits cannot be

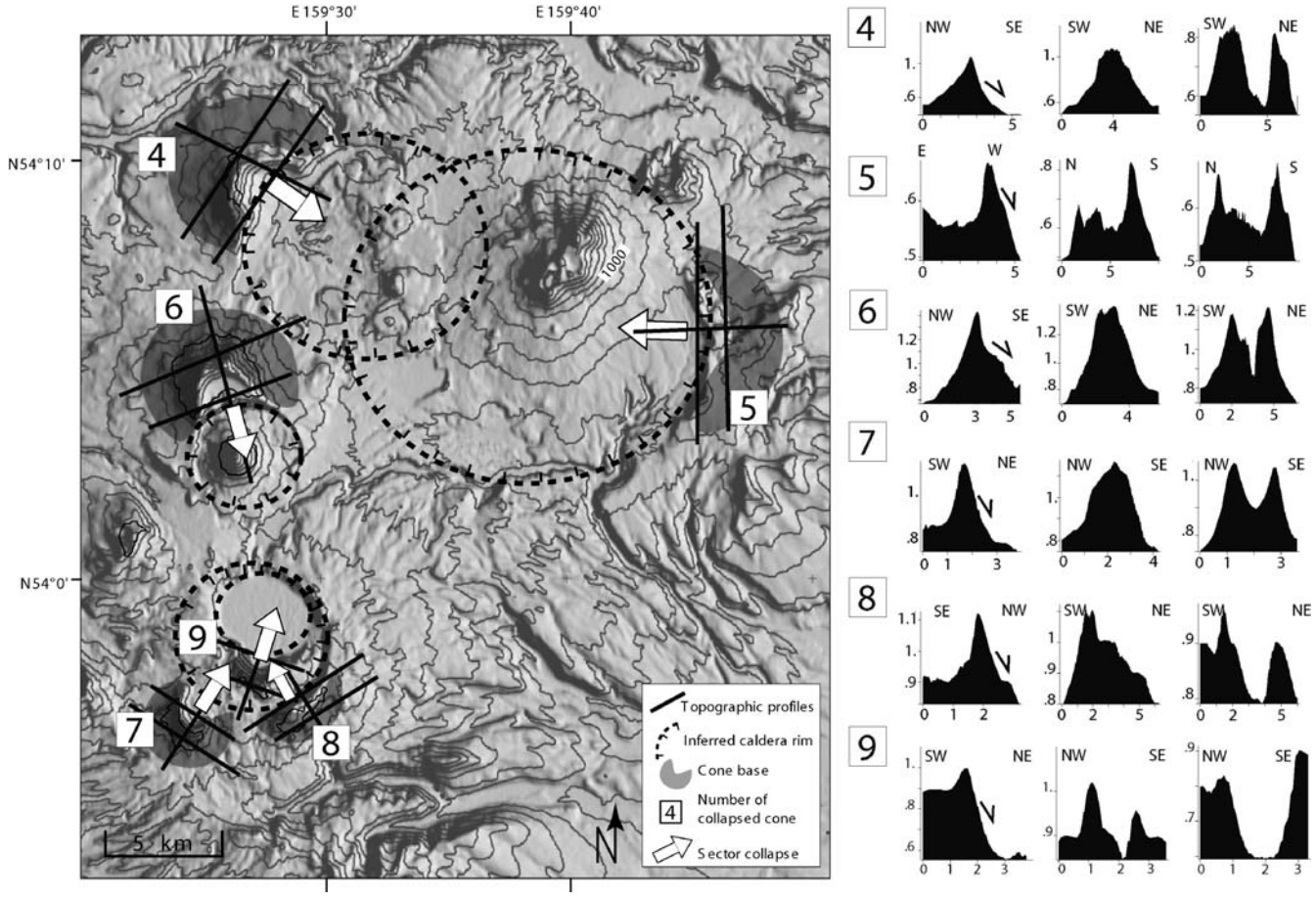

Fig. 3 Shaded relief map of calderas of the Karymsky region and topographic profiles through volcanoes located on the caldera boundaries. Names of volcanoes: *4* Soboliny, *5* Stena, *6* Dvor, *7* Belyankina, *8* Odnoboky, *9* Akademii Nauk. Symbols as on Fig. 2b. DEM from SRTM data, 100-m topographic isolines

observed now, as they are buried under thick caldera infill (syn-caldera ignimbrites and/or younger deposits). The characteristics of the calderas and the cones are summarized in Table 1. The present-day volume of remnant cones was calculated based on the digital elevation data of the volcano (cf. Figs. 2 and 3), while the pre-collapse volume of the cone was quantified by a Gaussian approximation of an ideal cone. Figure 4 illustrates the geometric determination and volume that approximates the pre-collapse cone for Stena volcano. By subtracting the present-day volume from pre-collapse volume, we can estimate the volume of the failed landslide mass which was deposited inside the caldera (see Table 1).

Although we have focussed our study on the Kamchatka Peninsula, the phenomenon of caldera/cone interaction is rather common in other volcanic regions that have calderas too. Well known examples include Fisher caldera (Aleutian Islands), Taal caldera (Philippines), Santorini (Greece), and Krakatau (Indonesia). Boundaries of these calderas have deep embayments that are in contact with remnants of pre-existing volcanic cones. The puzzling horseshoe-shaped morphology of Monte Somma (Italy), situated on the boundary of the caldera of Vesuvius, could also be the result of a large-scale landslide triggered by subsidence of the caldera.

Physical modeling

We conducted sand-box analogue experiments to test the hypothesis of giant failures of volcanoes caused by caldera subsidence, in order to understand the relationship between the position of a stratovolcano on a ring fault and the resultant degree and volume of volcano instability. An inflated sill-shaped rubber balloon of 20 cm plan view diameter was placed into a sand-box at 10 cm depth (Fig. 5). Small sand cones were placed on the flat sand surface eccentrically above the balloon in the vicinity of the expected "caldera fault" position. We then simulated ring faulting and caldera collapse by withdrawal of the balloon through a pipe system (cf. Walter and Troll 2001). We considered stratocones that were situated at various positions relative to the caldera faults: inside the caldera basin, above the caldera faults, or in the caldera periphery.

Table 1 Characteristics of the studied volcanoes and calderas situated in the central part of Kamchatka Peninsula

Volcanoes							Calderas		
Name	Age	Composition	Altitude (m)	Diameter of volcano base (km)	V reconstr/V current (km^3)	V lost (km^3/% of total volume)	Name	Diameter (km)	Age (Ka)
(1) Uzon	Late Pleisto.	B–A	800	5	3.9/2.3	1.6/41	Uzon	6×9	40
(2) Krasnaya sopka	Late Pleisto.	B–A	400	1.8	0.4/0.3	0.1/34	Uzon	-//-	-//-
(3) Ozernaya sopka	Late Pleisto.	B–A	300	5	1.3/0.4	0.9/69	Uzon	-//-	-//-
(4) Soboliny	L.Plio-M. Pleisto.	B–BA	550	7.2	7/4.8	2.2/31	Soboliny	9	180–140
(5) Stena	L.Plio-M. Pleisto.	B–BA	500	8	5/2.1	2.9/58	Stena	12	180–140
(6) Dvor	Late Pleisto.	BA	700	6.5	8.9/7.6	1.3/15	Karymskaya	5	7.9
(7) Belyankina	L.Plio-M. Pleisto.	B–BA–D	400	4	0.9/0.72	0.18/20	Odnoboky	4×6	110–80
(8) Odnoboky	L.Pleisto	BA–D	250	5	1.65/0.5	1.15/69	Odnoboky	-//-	-//-
(9) Akademii Nauk	L.Pleisto	D-R	250	2.7	0.2/0.48	0.28/58	Akademii Nauk	5×4	28–48

L.Plio late Pliocene, *M.Pleist* mid Pleistocene; *V* volume; *B* basalt, *A* andesite, *BA* basaltic andesite, *D* dacite, *R* rhyolite, *Alt* altitude, *V* volume. Ages and compositions of volcanoes and calderas after Ivanov 1970, Selyangin 1987, Ivanov et al. 1991, Leonov et al. 1991, Braitseva et al. 1995

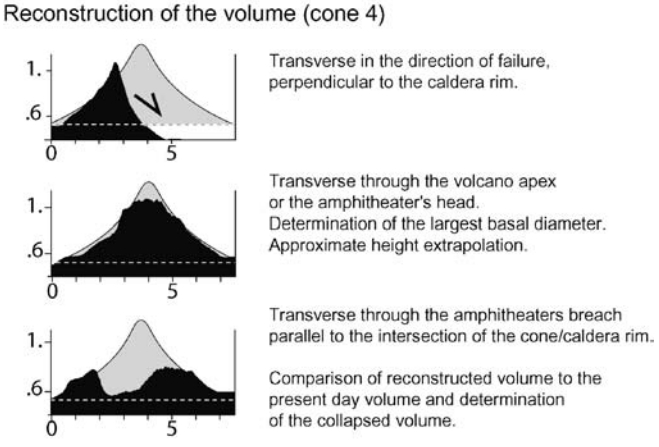

Fig. 4 Determination of volcano volume, illustrated for Stena volcano (cone 5 of Fig. 3). For simplicity a symmetric Gaussian shape (*rounded cone shape*) was assumed. The base of the edifice was set horizontally, the uniform radius defined manually, and height extrapolated

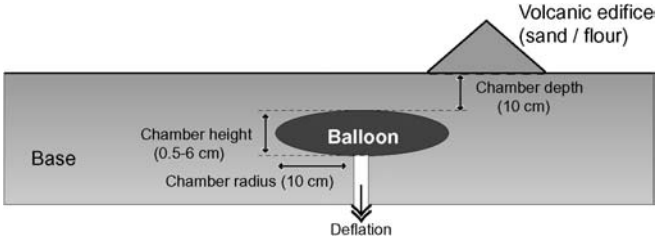

Fig. 5 Sketch of the experimental set-up. See text for details

Experimental procedure

In preliminary experiments we simulated pure caldera collapses to obtain the likely caldera dimensions. The way in which caldera collapse was accomplished was adapted from previous works (cf. Marti et al. 1994; Walter and Troll 2001). The inflated rubber reservoir was placed at specific depth of the sand-pile and then partially deflated to locate the position of the caldera faults. Then the experiment was repeated, however, this time small cones were constructed on the surface by pouring sand through a funnel. The small cones modeled volcanoes and were placed next to or above the predicted caldera faults. We then measured the cones. Upon caldera subsidence, which lasted several minutes, the cones were breached by faults, causing small caldera-directed landslides or frequently large slumps into the caldera basin (Fig. 6). The resultant geometry was again recorded and measured. Walter and Troll (2001) described two main circular faults of pure collapse calderas: an inner ring of reverse faults, surrounded by an outer normal fault region. We thus placed, in separate experiments, the pre-caldera cones at various positions where the surface expression of both fault types were expected. By changing one parameter, such as the cone position relative to the ring fault position, we obtain a first order approximation of the relationship between stratovolcano position and landslide volume transported into the caldera basin.

To allow direct comparison of the experiments with our field studies in Kamchatka, the analogue experiments were scaled to approximate realistic parameters. The procedure to obtain experimental similarity has been described in detail by the classic works of Hubbert (1937), Sanford (1959) and Ramberg (1981). For geometric scaling, all lengths must be scaled. Consequently, mechanical scaling of the experiments was also necessary, requiring much weaker materials as analogue medium. For a geometric scaling ratio of 1:100 000 (1 cm in the experiment equals approximately 1 km in nature), we used materials which are about 10^{-5} times weaker than natural rocks. Thus, modeling of natural caldera/cone interactions in Kamchatka (Table 1) required diameters of the modeled calderas from 5 to 15 cm. Caldera subsidence reached 0.5–2 cm in depth, and the basal diameters of the cones were 2–10 cm, and heights of the cones were 1–3 cm. Since the cohesive strength of upper crustal rocks

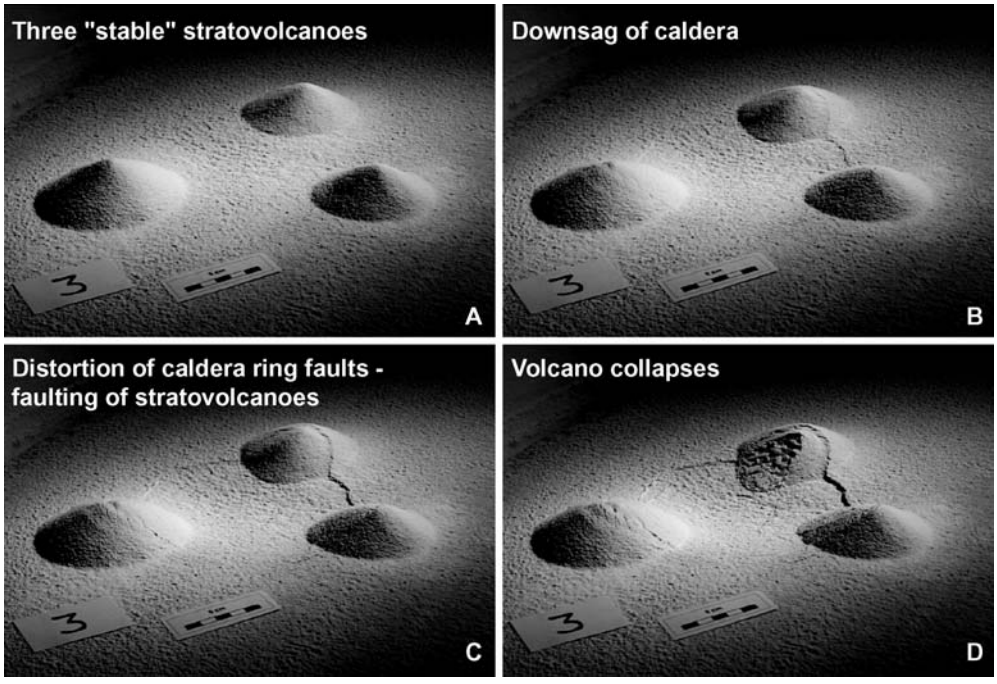

Fig. 6 Sand-box experiment showing development of a caldera with destabilization of volcanic cones situated eccentrically above the magma chamber. **A** before the caldera formation; **B** initial stage of caldera subsidence; formation of ring fault; **C** intermediate stage; the ring fault crosscuts the volcanic cones. **D** final stage of the caldera subsidence; strong destabilization of the cones causes sectors to collapse toward the forming caldera basin

ranges from 10^6 to 10^7 Pa (e.g. Schultz 1996), we performed the same experiments for two different analogue materials, in order to guarantee the general validity of the deformation described herein. In the first set of experiments, a mixture of dry eolian sand and flour in a proportion of 10:1 simulated more cohesive rocks. The cohesion of this mixture is in the range of 100–500 Pa, so that fault positions and their orientations are clearly observable in plan view without model destruction. These experiments were then repeated using dry sand only as the analogue crustal material. Sand, having very low cohesion, approximates a linear relation of shear stress and normal stress by the Coulomb criterion of brittle failure (Ramberg 1981).

For both materials, the friction coefficient is quasi-invariant, having values of 30° (sand) and 35° (sand flour mixture) for the angle of internal friction, which are both compatible with 30–35° for natural cones. Mean densities of rocks are on the order of 2,750 kg/m^3, while the experimental materials were between 1,700 kg/m^3 (sand) and 1,400 kg/m^3 (sand-flour). The experimental materials and scaling are described in more detail in Walter and Troll (2001).

Necessary simplifications of the experiments were as follows: The gravitational acceleration was not scaled. Also, using a balloon as an analogue for magma chambers prevents blocks from sinking into the chamber. Although these factors may limit realistic caldera behaviour to some extent, this setup was ideal for our purpose, since we knew the actual dimensions of the reservoir and thus the likely positions of ring faults.

Experimental results

Our results show that a single caldera fault, when propagating through a volcanic cone, splits into two faults. Stratovolcanoes situated above a caldera fault are thus separated into three domains: a stable external part on the footwall block, an unstable part on the hanging wall, and a central wedge-like graben between (Fig. 7). The main displacement within the cone was along the fault that separated the central block and the outer stable cone (Fig. 8). Occasionally parts of the central block and the inner part of the cone slid into the caldera basin, leaving a horseshoe-shaped scar (amphitheater) in the remnant cone. Similar behavior of a tectonic fault crossing a volcanic cone was observed in the experiments of Vidal and Merle (2000) and Merle et al. (2001). Cones deformed in a similar fashion above the inner reverse faults of the caldera and further outwards above the inward dipping peripheral normal faults; the general trisection of the stratocone was observed in all experiments. We measured the opening angle α of the amphitheater that formed by this faulting in order to describe this effect quantitatively (Fig. 9).

To understand the general geometric relations between a stratovolcano and a crossing caldera fault that gives rise to flank instability, we used a parameter D^*, which is defined as the initial diameter of the base of the cone D_I, divided by the remnant diameter of the base of the cone D_{II} that is unaffected by caldera faulting (Fig. 9). The value D^* is hence 1 for stable cones that are positioned far outside the edge of a caldera. For cones that are separated by a caldera fault the value D_{II} decreases, according to $D^* = D_I / D_{II}$. We measured these values for more than 80 individual experiments, obtaining a wide range of D^* from 1 to about 25. For the highest D^* values, almost all

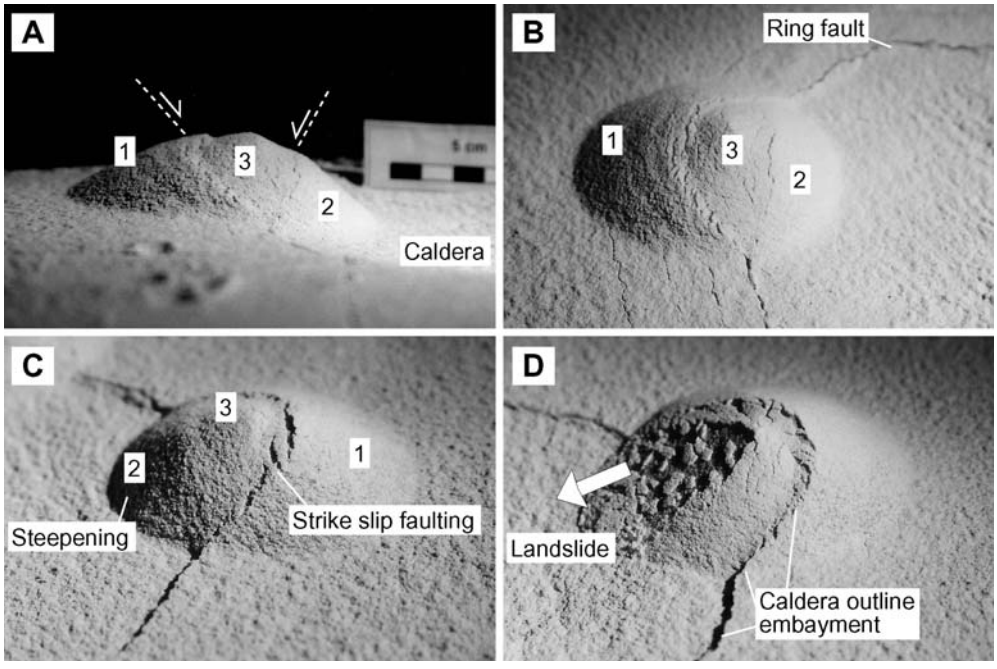

Fig. 7 A–D Sand-box model of morphological changes and structural segmentation of volcanic cones affected by the caldera ring fault. Perspective views of the individual cones, showing details of the morphological changes. Main structural sectors are a stable outer zone (*1*), a highly unstable and sliding inner zone (*2*), and a subsiding graben structure (*3*) between sectors (*1*) and (*2*). Note outward embayments of the caldera ring fault where it crosses the pre-caldera cones. In **C**, strike slip displacement forms en echelon fractures on the cone. In **D**, part of the same cone has collapsed into the caldera

of the cone subsided into the caldera. Fig. 9 summarizes our experimental data, showing a positive correlation between D^* and the opening angle α. The different analogue materials we used (pure sand and a sand/flour mixture) produced similar results, strengthening the general geometric validity of the experiments. Cones that are affected only at the margin by caldera faulting (small D^* values <1.5) produced a narrow horseshoe amphitheater, with the angle significantly smaller than 120°. By contrast, cones affected by more than 50% by ring faulting (D^* values >2) produced significantly broader amphitheaters. For D^* values >4 the opening angle of the "scar" increases to about 180°, resulting in a cone that is truncated in an almost linear fashion.

The experiments thus show that the curvature of caldera faults can be strongly modified by preexisting stratovolcanoes as defined by the D^* value. A cone affected to a minor degree by caldera subsidence (small D^*) develops a prominent narrow embayment into the cone. By contrast, a cone initially situated mostly inside the subsequent caldera results in a less curved caldera fault. These structural relationships are also found for the studied calderas of Kamchatka.

Discussion

The mechanism of caldera formation is a subject of much debate. Currently there is agreement that the principal process of formation of large calderas is rapid roof subsidence into shallow magma chambers due to large-scale eruptions (Walker 1984; Lipman 1997). The subsidence can occur in several ways (e.g. piston, piecemeal, trapdoor), with downward vertical movements of blocks of a roof, or the roof as a whole, as the main feature common to all calderas (Walker 1984). Lavallée and coworkers (2004) found that the style of caldera subsidence can be influenced by the preexisting loading conditions (i.e. the topography). Accordingly, the topographic load exerts some control on the pattern of subsidence. The effect of a non-planar free surface also may influence the stress trajectories and caldera fault formation. Landsliding frequently occurs from the oversteepened caldera walls during and after caldera formation (e.g. Lipman 1997; Druitt et al.1999). Our study has shown that caldera subsidence preferentially destabilizes nearby volcanic cones and topographic highs, which have formed during pre-caldera activity. This process has led, in many cases, to large-scale failures of the caldera-facing flanks of the cones, with material sliding into the caldera basin (Fig. 10). The accumulation of material filling in a caldera, i.e. by ignimbrites and lateral mass wasting, is thus a complex process.

A comparison of geometries of the remnants of volcanic cones destabilized by caldera subsidence events in Kamchatka with the data obtained from our sand-box experiments shows good agreement (Fig. 9). Volcanic cones situated mostly outside the caldera ring faults are affected by caldera subsidence to minor degrees only, such as the cones of Belyankina and Krasnaya Sopka volcanoes. These formed narrow amphitheaters deeply incised into the cones. Cones which occur mostly inside circular caldera faults, such as Stena and Ozernaya Sopka volcanoes, collapsed with formation of very broad amphitheaters. The only volcano that differs significantly from the experimental data is Dvor. This is because Dvor had been decapitated and had failed prior to subsidence of Karymskaya caldera (Ivanov 1970). The absence of the cone's top reduced gravitational stresses inside the edifice of the volcano, resulting in a rather small destabilized

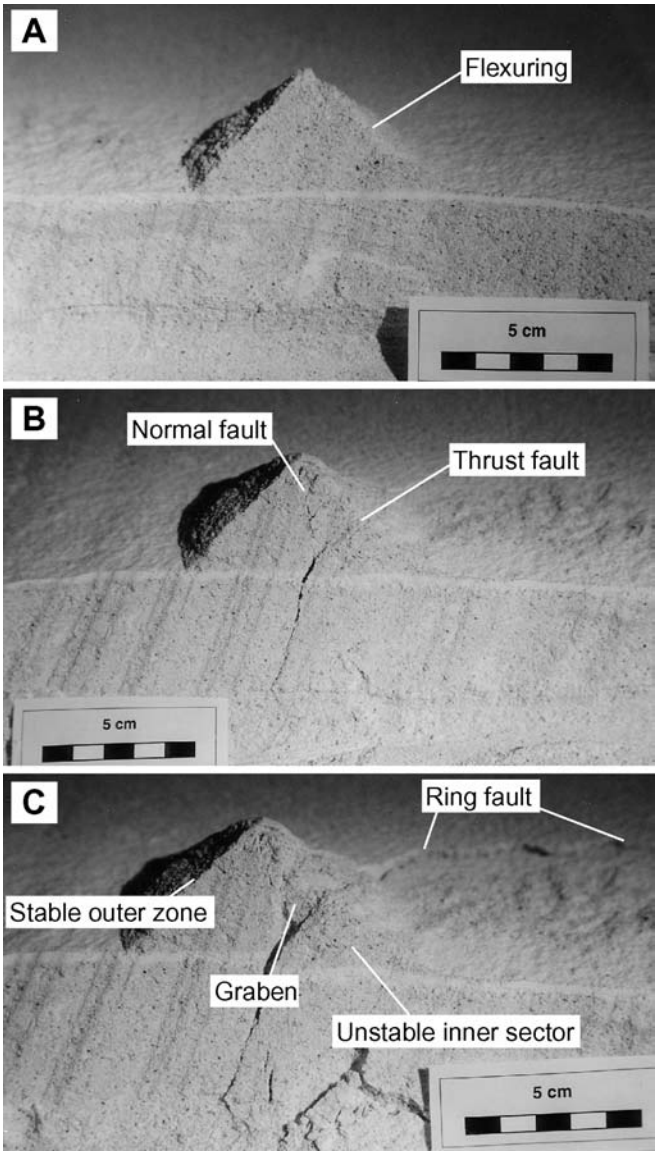

Fig. 8 Cross sections of a sand-box/flour model showing development of inner structure of a volcanic cone destabilized by the caldera ring fault. **A** incipient stage of subsidence of the caldera; **B** intermediate stage; **C** fully developed

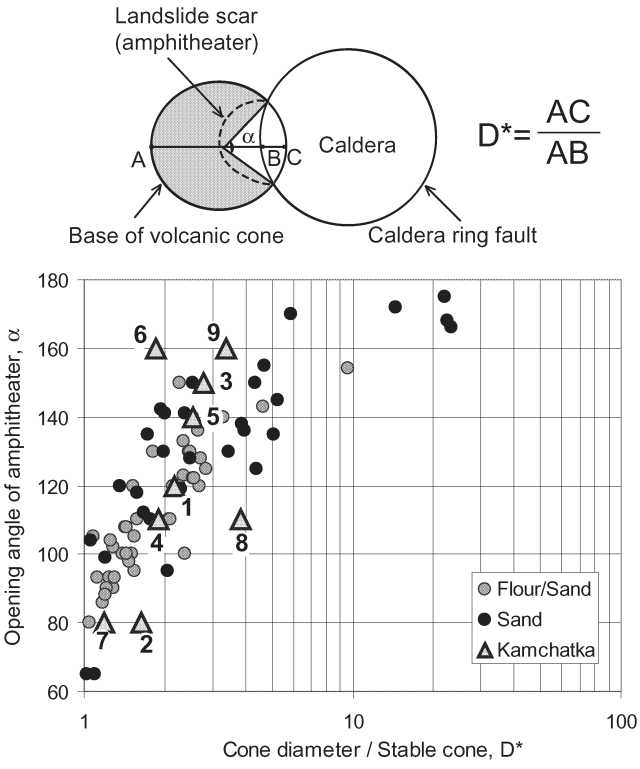

Fig. 9 Relationship between the relative position of caldera faults under destabilized cones (*expressed as cone diameter/stable cone ratio*) and the opening angle of the resulting landslide scars (*amphitheaters*) for experimental and Kamchatkan data. *Numbers* indicate volcanoes: *1* Uzon, *2* Krasnaya Sopka, *3* Ozernaya Sopka, *4* Soboliny, *5* Stena, *6* Dvor, *7* Belyankina, *8* Odnoboky, *9* Akademii Nauk. Determination of the parameters used for the plot are shown on the inserted sketch. *AC* cone diameter (initial diameter at the base of a pre-caldera volcanic edifice); *AB* stable cone diameter (diameter of the stable part of a cone base); α opening angle of the landslide scar

sector and the formation of an amphitheater having an unusually large opening angle. This example shows that our proposed relationship works best for volcanic edifices with initial pre-caldera morphologies close to a regular cone.

Our study also shows that the volume of material which deposits into a caldera basin may be significant. For the studied individual cones in Kamchatka, this volume reached up to 2.9 km^3 (Table 1). Since some pre-caldera cones can be very large, landslide volumes may reach several tens of km^3. Destabilization of the experimental cones occurred as soon as the caldera faults formed. This implies that a stratocone sector collapse may occur during the early stages of caldera subsidence. The resulting debrites are thus likely to be deposited at or near the base of the intra-caldera stratigraphy, and may become mixed with pyroclastic eruptive deposits. The amount of lithic fragments in the pyroclastic caldera stratigraphy may thus be highly variable through an intra-caldera succession. Distinguishing between landslides from sector failure of cones and "normal" landslides from unstable caldera walls is challenging. We conjecture that due to the higher slope steepness and kinetic energy the cones are structurally more unstable than the caldera walls, and thus deposit early during caldera evolution in form of landslides with longer run out distances.

Although we could not model transformation of the landslides into debris avalanches and their transport and deposition into the caldera with our experimental setup, we deduce that such avalanches would have high mobility similar to debris avalanches produced by non-caldera-related sector collapses of volcanoes (Voight 1981; Siebert 1984; Belousov 1995; Belousov and Belousova 1996; Glicken 1998). High mobility debris avalanches could travel long distances across caldera basins. Thus, although vertical movements of blocks dominate in caldera-forming processes, horizontal transport of material is also

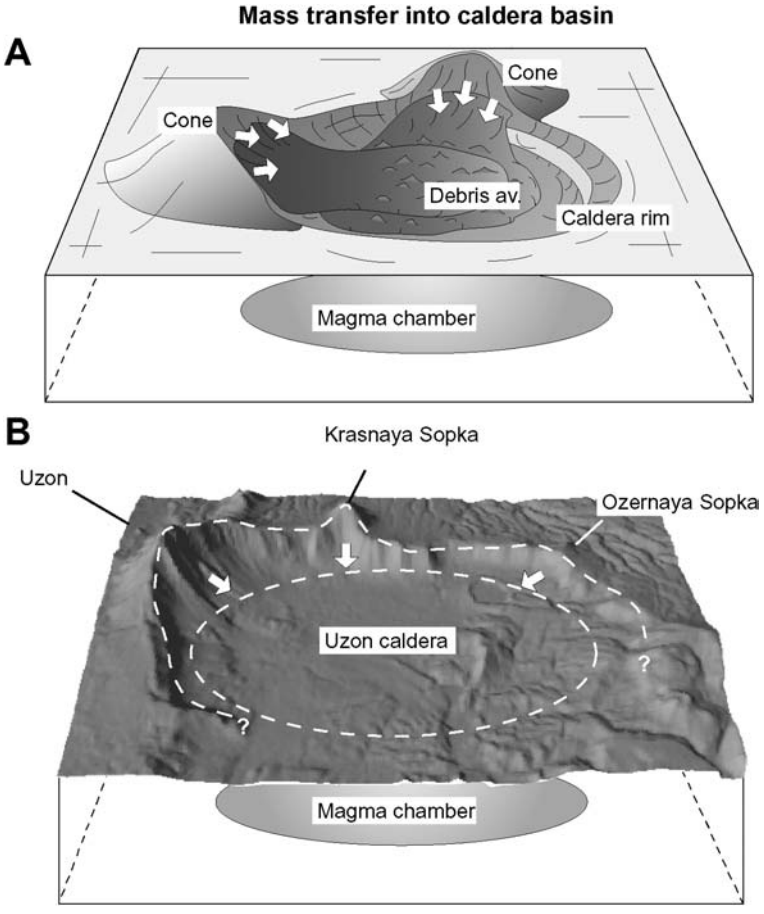

Fig. 10 Sketches showing the process of caldera subsidence and destabilization of volcanic cones situated on caldera ring faults. **A** Perspective illustration of the proposed model of caldera formation with large-scale landslides developing from the pre-caldera cones. The landslides generate debris avalanches that deposit material in the caldera basin. **B** Perspective view of digital elevation data and application of the model to the formation of Uzon caldera

important in cases where large cones are destabilized by caldera subsidence (see Fig. 10).

The internal parts of youthful calderas are generally poorly exposed, and thus few data exist regarding intracaldera fill and structures. We know about small-scale landslides that occur into caldera basins, but little documentation exists regarding large-scale syn-caldera debris avalanche deposits. Postulated debris avalanches in the studied calderas of Kamchatka cannot be observed as they are buried under thick caldera infill. An important feature of syn-caldera debris avalanches may be their simultaneous deposition with voluminous pyroclastic flows, implying that intermixing with ignimbrite material is likely to occur (cf. Lipman 1976; Troll et al. 2000).

In turn, topographic margins of large calderas are commonly not perfectly circular or elliptical, but frequently have one or more large outward embayments. We suggest that if such embayments represent horseshoe-shaped amphitheaters within pre-caldera volcanic cones, they are likely to represent scars of large-scale landslides off the cones, which formed contemporaneous with caldera formation. Thus, the scalloped appearance of many caldera boundaries can be explained by the influence of topography on the process of caldera formation, without the need to invoke complex geometries of magma chambers, several episodes of caldera-forming eruptions, or modification by post-caldera erosion.

In our experiments, large landslides occurred only where caldera boundaries intersected cones. At places where cones were absent and the pre-caldera surface was flat, caldera walls were comparatively stable. This explains why some natural calderas have no prominent outward embayments. During the formation of calderas, numerous small-scale landslides may occur, but large-scale landslides play probably a relatively minor role for normal caldera walls lacking preexisting topographic relief.

Gravitational instability of volcanic cones and their susceptibility to large-scale sector collapses is now widely accepted (e.g. Siebert 1984). Several triggering mechanisms have been recognized, including (1) intrusions of magma, (2) changes of water table, (3) seismicity, and (4) movements along tectonic faults in the volcano's basement (Belousov et al. 1999; Vidal and Merle 2000). A relationship of cyclic caldera events and flank instability was proposed by Walter and Troll (2001) and for ocean islands by Troll et al. (2002); in these scenarios, landslides are directed outward along the periphery of a caldera. This study has shown that interaction of a volcanic cone with a caldera ring fault is another common mechanism of destabilization of volcanoes, resulting in large-scale failures directed into the caldera basin.

The phenomenon of failures of volcanoes on the boundaries of forming calderas has probably no direct application for volcanic hazard assessments because the

effects from caldera-forming eruptions themselves exceed those from associated edifice failures. Indirect hazards can be associated with tsunamis generated by cone failures in cases where caldera-forming eruptions occur in marine environments. Indeed, it is well known that transport of a volcanic debris avalanche into the sea causes large tsunami (Latter 1981; Kienle et al. 1987). The only historical example of the formation of a submarine caldera was Krakatau in 1883, which generated a series of deadly tsunami (Francis 1985). During this eruption, several mechanisms may have been responsible for generation of tsunami: earthquakes, explosions, caldera subsidence, and deposition of pyroclastic flows (Latter 1981), but large-scale landslides of pre-caldera cones, such as Rakata volcano, may have also generated tsunami (Francis 1985). Large tsunami were also produced during the Minoan caldera-forming eruption of Santorini around 1500 B.C. (Druitt et al. 1999). The morphology of this submarine caldera suggests that its formation caused destabilization and inward sliding of pre-caldera cones, which may have generated the largest tsunami. We therefore speculate that the presence of large cones in the vicinities of developing submarine calderas increases the potential of large tsunami hazards.

Conclusions

1. Shapes of calderas strongly depend on pre-caldera topography.
2. Subsidence of a caldera destabilizes peripheral pre-caldera volcanic cones and triggers large-scale cone failure with formation of amphitheaters facing the caldera basin. A geometric relationship between opening angle of the formed amphitheater and the relative position of the cone edifice above the caldera fault exists.
3. Debris avalanches originating from pre-caldera cones can play a significant role in caldera-forming processes and contribute substantially towards the fill of a caldera basin.

Acknowledgements A. Belousov thanks the Russian Foundation of Basic Research, which supported this study, and funding by the Alexander von Humboldt Foundation during his stay at the Dept. of Volcanology and Petrology at GEOMAR, Germany. T.R. Walter was supported by a grant of the Deutsche Forschungsgemeinschaft (WA1642–1/2) and V.R. Troll through a travel grant by Trinity College to visit GEOMAR. Special thanks to M. Belousova for final preparation of the manuscript. Reviews by J. Stix and J. Lavallée helped to improve the manuscript.

References

Acocella V, Cifelli F, Funiciello R (2001) The control of overburden thickness of resurgent domes: insights from analogue models. J Volcanol Geotherm Res 111:137–153

Belousov A (1995) The Shiveluch volcanic eruption of 12 November 1964—explosive eruption provoked by failure of the edifice. J Volcanol Geotherm Res 66: 357–365

Belousov A, Belousova M (1996) Large scale landslides on active volcanoes in XXth century—examples from Kurile-Kamchatka region (Russia). In: Senneset K (ed) Landslides. Balkema, Rotterdam pp 953–957

Belousov A, Belousova M, Voight B (1999) Multiple edifice failures, debris avalanches and associated eruptions in the Holocene history of Shiveluch volcano, Kamchatka, Russia. Bull Volcanol 61:324–342

Braitseva OA, Melekestsev IV, Ponomareva VV, Sulerzhitsky LD (1995) Ages of calderas, large explosive craters and active volcanoes in the Kuril-Kamchatka region, Russia. Bull Volcanol 57:383–402

Branney MJ (1995) Downsag and extension at calderas: new perspectives on collapse geometries from ice-melt, mining and volcanic subsidence. Bull Volcanol 57:303–318

Druitt DH, Sparks RSJ (1984) On the formation of calderas during ignimbrite eruptions. Nature 310:679–681

Druitt TH, Edwards L, Mellors RM, Pyle DM, Sparks RSJ, Lanphere M, Davies M, Barriero B (1999) Santorini volcano. Geol Soc Lond Mem 19:1–165

Francis PW (1985) The origin of the Krakatau tsunamis. J Volcanol Geotherm Res 25:349–364

Francis PW (1993) Volcanoes: a planetary perspective. Clarendon Press, Oxford, pp 1–443

Glicken G (1998) Rockslide-debris avalanche of May 18, 1980, Mount St. Helens volcano, Washington. Bull Geol Soc Jpn 49:55–105

Hubbert M (1937) Theory of scale models as applied to the study of geologic structures. Geol Soc Am Bull 48:1459–1520

Ivanov BV (1970) Eruption of Karymsky volcano in 1962–1965 and volcanoes of Karymsky group (in Russian). Nauka, Moscow, pp 1–134

Ivanov BV, Braitseva OA, Zubin MI (1991) Karymsky volcano. In: Fedotov SA, Masurenkov YuP (eds) Active volcanoes of Kamchatka. vol. 2, Nauka, Moscow, pp 182–203

Kennedy B, Stix J, Vallance JW, Lavallée Y, Longpré M-A (2004) Controls on caldera structure: results from analogue sandbox modeling. Geol Soc Am Bull 116:515–524

Kienle J, Kowalik Z, Murty TS (1987) Tsunamis generated by eruptions from Mount St. Augustine volcano, Alaska. Science 236:1142–1147

Komuro H (1987) Experiments of cauldron formation: a polygonal cauldron and ring fractures. J Volcanol Geotherm Res 31:139–149

Latter JH (1981) Tsunamis of volcanic origin: summary of cases with particular reference to Krakatoa, 1883. Bull Volcanol 44:467–490

Lavallée Y, Stix J, Kennedy B, Richer M, Longpré M-A (2004) Caldera subsidence in areas of variable topographic relief: results from analogue modeling. J Volcanol Geotherm Res 129:219–236

Leonov VL, Grib EN, Karpov GA et al. (1991) Caldera Uzon and Valley of Geysers. In: Fedotov SA, Masurenkov YP (eds) Active volcanoes of Kamchatka. vol. 2, Nauka, Moscow, pp 94–137

Lipman PW (1976) Caldera-collapse breccias in the western San Juan Mountains, Colorado. Geol Soc Am Bull 87:1397–1410

Lipman PW (1997) Subsidence of ash flow calderas: relation to caldera size and chamber geometry. Bull Volcanol 59:198–218

Marti J, Ablay GJ, Redshaw LT, Sparks RSJ (1994) Experimental studies of collapse calderas. J Geol Soc Lond 151:919–929

Merle O, Vidal N, Van Wyk de Wries B (2001) Experiments on vertical basement fault reactivations below volcanoes. J Geophys Res 106:2153

Newhall C, Dzurisin D (1988) Historical unrest at large calderas of the world. US Geol Surv Bull 1855:1–1108

Newhall C, Punongbayan R (eds) (1996) Fire and mud: eruptions and lahars of Mount Pinatubo, Philippines. University of Washington Press, Seattle, pp 1–1126

Piip BI (1961) Kronotskie ignimbrites at Kamchatka. Tr Lab Vulc AN USSR 20

Pinel V, Jaupart C (2003) Magma chamber behavior beneath a volcanic edifice J Geophys Res 108(B2), 2072, DOI:10.1029/2002JB001751
Ramberg H (1981) Deformation structures in theory and experiments. Geol Soc Swed pp 1–131
Roche O, Druitt T, Merle O (2000) Experimental studies of caldera formation. J Geophys Res 105:395–416
Sanford A (1959) Analytical and experimental study of simple geological structures. Geol Soc Am Bull 42:19–52
Schultz RA (1996) Relative scale and the strength and deformability of rock masses. J Struct Geol 18:1139–1149
Seibert L (1984) Large volcanic debris avalanches: characteristics of source areas, deposits, and associated eruptions. J Volcanol Geotherm Res 22:163–197
Selyangin OB (1987) Petrogenesis of basalt-dacites in the connection with evolution of volcano-structures (in Russian). Nauka, Moscow, pp 1–148
Simkin T, Fiske RS (1983) Krakatau 1883: The volcanic eruption and its effects. Smithsonian Institution, Washington, DC, 494 pp
Troll VR, Emeleus CH, Donaldson CH (2000) Caldera formation in the Rum Igneous Complex, Scotland. Bull Volcanol 62:301–317
Troll VR, Walter TR, Schmincke H-U (2002) Cyclic caldera collapse: piston or piecemeal subsidence? Field and experimental evidence. Geology 30:135–138
Vidal N, Merle O (2000) Reactivation of basement faults beneath volcanoes: a new model of flank collapse. J Volcanol Geotherm Res 99:9–26
Voight B, Glicken G, Janda RL, Douglass PM (1981) Catastrophic rockslide avalanche of May 18. In: Lipman PW, Mullineaux DR (eds) The 1980 eruptions of Mount St. Helens, Washington. US Geol Surv Prof Pap 1250:347–378
Walker GPL (1984) Downsag calderas, ring faults, caldera sizes and incremental growth. J Geophys Res 89:8407–8416
Walter TR, Troll VR (2001) Formation of caldera periphery faults: an experimental study. Bull Volcanol 63:191–203
Williams H (1941) Calderas and their origin. Univ Calif Publ Bull Dep Geol Sci 25:239–346